

1 Supplemental Materials

2 Total Performance of Magneto-Optical Ceramics with 3 a Bixbyite Structure

4 Akio Ikesue ¹, Yan Lin Aung ^{1,*}, Shinji Makikawa ², and Akira Yahagi ²

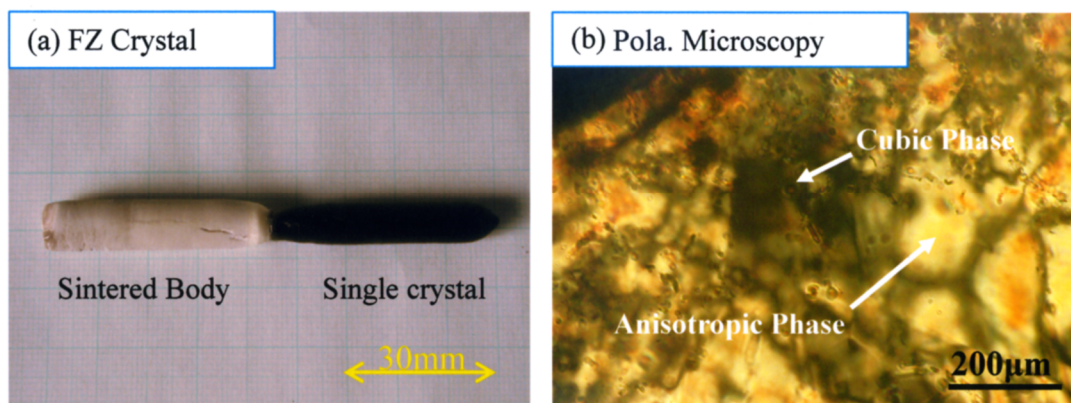
5 ¹ World-Lab. Co., Ltd., Mutsuno, Atsutaku, Nagoya 456-0023, Japan; poly-ikesue@s5.dion.ne.jp

6 ² Shin-Etsu Chemical Co., Ltd., Advanced Functional Materials Research Center, Matsuida, Annaka, Gunma
7 379-0224, Japan; s_makikawa@shinetsu.jp (S.M.); yahagi@shinetsu.jp (A.Y.)

8 * Correspondence: poly-yan@r2.dion.ne.jp

9 Fabrication of Single Crystal TYO by FZ Method

10 A single crystal TYO was grown by conventional melt growth method and technical issues were
11 discussed. An external view of $(\text{Tb}_{0.5}\text{Y}_{0.5})_2\text{O}_3$ single crystal grown by FZ method is shown in Figure
12 S1(a). Firstly, powder compact having a composition of Tb_4O_7 (50 mol%)- Y_2O_3 (50 mol%) was sintered
13 under Ar-3\%H_2 atmosphere for 2 h at 1500 °C, and then it was grown by the FZ (floating zone) method
14 (crystal growth rate 5 mm/h, rotation speed 30 rpm, and atmosphere Ar-8\%H_2). Internal
15 microstructure was observed under transmission polarized optical microscope (see Figure S1(b)). It
16 was not homogeneous. Voids, cracks, double refractions and inclusions were observed in all positions
17 of the crystal. The crystal structure of this material at room temperature is a cubic system. However,
18 during cooling process after melting at 2400 °C phase transition occurred from hexagonal \Rightarrow
19 orthorhombic \Rightarrow cubic crystal system. Therefore, some parts were not confirmed as dark-field under
20 cross nicols due to the formation of optically anisotropic phases. Insertion loss (I.L.) and extinction
21 ratio (E.R.) were measured (sample thickness: 5mm). The average values of insertion loss (I.L.) and
22 extinction ratio (E.R.) were 2.57 dB and 10.6 dB, respectively, which imply very high optical loss and
23 very small extinction ratio. Therefore, it is noteworthy that even a single crystal TYO produced by
24 melt-growth method cannot provide a good optical quality with practical size for this kind of isolator
25 material.



26

27 **Figure S1.** (a) External view, and (b) polarized optical microscopic image of $(\text{Tb}_{0.5}\text{Y}_{0.5})_2\text{O}_3$ single crystal.

28 Characterization on TYO Ceramics

29 Thermal weight analysis and differential thermal analysis (TG-DTA) of the starting powder
30 (Tb_4O_7) were performed using Rigaku (Thermo Plus EVO TG8120) with a heating rate of 15 °C/min
31 in flowing air. SEM images were obtained with a JEOL scanning electron microscope (JSM-7000F)
32 operated at 10kV. TEM images were acquired with a JEOL spherical aberration corrected Scanning
33 Transmission Electron Microscope (Cs-corrected STEM, ARM-200F) operated at 200kV. Samples for
34 TEM analysis were prepared as follow. A sample with 3 mm diameter was cut out by ultrasonic

35 processing after making a thin sheet of sample by diamond polishing. Then the center part of the
36 sample was polished down to about 20 μm by a dimpler, and finally finished up by Ar-ion milling
37 (GATAN PIPS). In order to prevent charge-up issue, carbon deposition was done on the surface of
38 the finished samples. Transmission polarized optical microscopic images were obtained using an
39 Olympus BX50 attached with polarizer plate. Transmission and absorption spectra were measured
40 by using a spectrophotometer (JASCO, V-670). Optical-polished samples with a thickness of 5mm
41 were used. Polarized image was obtained by using a macro polarizer (TOSHIBA, SVP-200).
42 Variations in refractive index for the whole position of each ceramic sample were observed by using
43 a Schlieren photography system (Mizojiri Kogaku, SLM-10S). Optical wavefront distortion was
44 measured at 632nm using an interferometer (GPI-XP, Zygo Ltd., USA). Optical polished samples with
45 surface flatness better than $\lambda/10$ was used for this measurement. Infrared DPSS laser (Sanctity Laser,
46 1064 nm) with Gaussian mode was irradiated into the sample. Then the transmitted laser beam
47 pattern was recorded on a beam profiling camera (Spiricon, SP620U).

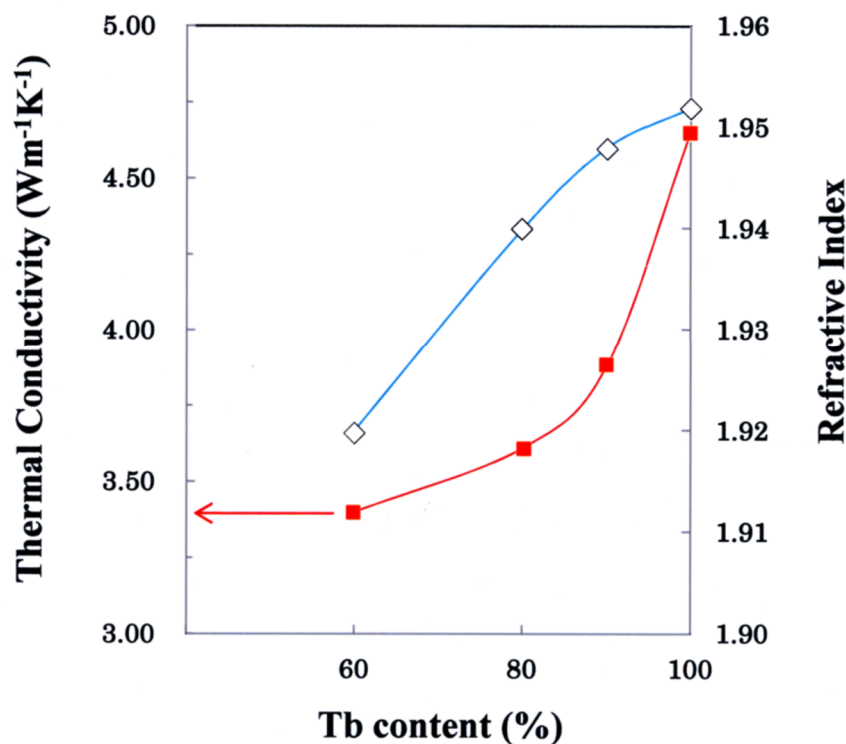
48 The Verdet constant was determined by the following method. 20.0mm long TGG crystal
49 (Electro-Optics Technology Inc.) and 8.0 mm long $(\text{Tb}_{0.6}\text{Y}_{0.4})_2\text{O}_3$ (abbr. as "TYO") ceramics were used
50 as Faraday rotator in this measurement. The outer diameter of each sample was 5.0mm. The Faraday
51 rotator sample was placed inside a hollow cylinder magnet (Nd-Fe-B, Shin-etsu Chem. Co.) such that
52 the sample is located at the center of light axis. The wavelength of light source (cw laser diode, 10mW,
53 FiberLabs Inc. FPLD-1060-24) with 1064 nm was irradiated into the Faraday rotator along the light
54 axis. The Faraday rotation angle of the output laser beam was measured to be 45.0 degree by using
55 polarizer plates. The distribution of magnetic field intensity was calculated by finite element method
56 (JMAG-Designer). Magnetic field intensity applied to each sample was 0.98 T for 20 mm long TGG
57 crystal and 1.12T for 8.0 mm long TYO ceramics, respectively. From the above measurement results,
58 Verdet constants were determined by the following formula: $\theta_F = VHL$, where is Faraday rotation
59 angle, H is magnetic field intensity, and L is length of the Faraday rotator.

60 Thermal conductivities of each ceramic sample were measured by laser flash method using an
61 Advance-Riko TC-7000. Triangular prisms were used and minimum angle of deviation method was
62 applied to calculate the refractive index (Möller-Wedel GmbH, Gonio-Spectrometer Type II). Output
63 power of 50 W laser (1070nm wavelength, cw single mode ytterbium fiber laser manufactured by IPG
64 photonics corp.) was used as a light source to evaluate the thermal lens effect of the materials. Due to
65 thermal lens effect, generally beam shape is slightly deformed after passing through a sample.
66 Change in beam waist of laser beam after passing through each sample was measured as thermal
67 lens effect index by using a beam profiler (Coherent Inc.). In power handling test, pulsed laser (pulse
68 width 50 ps, peak power 0.3 MW, beam spot Φ 0.7 mm, power density 78 MW/cm²) was irradiated
69 into the optical polished sample at 2 MHz for 7000 h, and inspected the condition of the irradiated
70 sample.

71 To evaluate Faraday rotation performance, a continuous wave (cw) laser diode (FiberLabs Inc.
72 FPLD-1060-24) was used as an incident laser source (1064nm, max. output 10 mW). Laser was
73 irradiated onto the sample, which is placed between input polarizer and output analyzer made of
74 Glan Thompson prism (GTP). The extinction ratio of the prism was 50 dB. The samples of $(\text{Tb}_{0.6}\text{Y}_{0.4})_2\text{O}_3$
75 ceramics (5 mm in diameter by 8 mm length) and TGG single crystal (5 mm in diameter by 20mm
76 length, Electro-Optics Technology Inc.) with $\langle 111 \rangle$ orientation were used. Each sample was clamped
77 in copper holder and commercial Faraday rotator magnetic housing was used. Nd-B paramagnets
78 (Shin-Etsu Chem. Co.) were used to generate high axial magnetic field. Magnetic field applied to TGG
79 crystal and $(\text{Tb}_{0.6}\text{Y}_{0.4})_2\text{O}_3$ ceramics was 0.98 T and 1.12 T, respectively. A polarization plane of incident
80 laser light was rotated by the Faraday effect because of the magnetic field. The transmitted laser
81 output was measured by using a power meter with respect to each rotation angle of output polarizer
82 ranging from -45 to 135 degree.

83 Relationship between the Tb Ion Content and Refractive and Thermal Conductivity

84 Figure S2 shows the relationships between the concentration of Tb ions in TYO ceramics and the
 85 refractive index, and the thermal conductivity. The thermal conductivity for Tb = 50~100 % regions is
 86 about 3.3–4.6 Wm⁻¹K⁻¹, which is comparable to that of the commercial TGG or TAG single crystals.

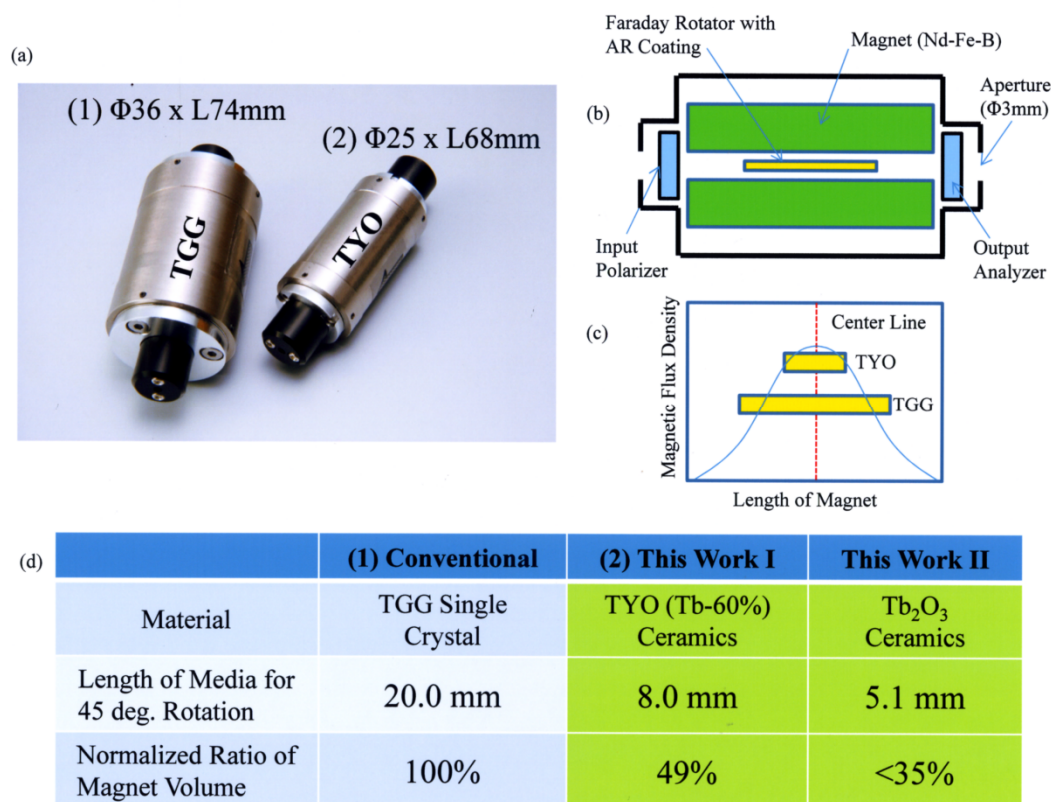


87

88 **Figure S2.** Relationships between the Tb ion concentration and the refractive index, and the thermal
 89 conductivity.

90 Demonstration of Optical Isolator Device Using the TYO Ceramics

91 Prototype of optical isolator using TYO (Tb-60%) ceramic is shown in Figure S3(a) in comparison
 92 with commercial TGG optical isolator. Schematic diagram of general optical isolator is shown in
 93 Figure S3(b). It is simply made of an input polarizer (polarized vertically), a Faraday rotator element,
 94 and an output polarizer. An AR-coated Faraday rotator element is placed inside an Nd-Fe-B
 95 permanent magnet (a hollow cylinder magnet) such that the element is located at the center of light
 96 axis. The angle between the input polarizer and the output polarizer is set to 45°. The Faraday rotator
 97 is selected to provide a 45° rotation angle with a certain length. As for TGG crystal, it requires 20.0mm
 98 length. As for TYO (Tb = 60%) ceramic sample, it requires 8.0mm length in the same magnetic field.
 99 As illustrated in Figure S3(c), magnetic flux density decreased with the distance from the center line.
 100 Therefore, magnetic field can be more effectively used by placing a shorter element with larger Verdet
 101 constant in the case of same magnet house. In other words, as shown in the Figure S3(a), it is possible
 102 to produce with smaller magnet house (about half-size by volume) by using the TYO ceramics with
 103 larger Verdet constant, leading to miniaturization and low cost at the same time. The features of each
 104 Faraday rotator material are summarized in Figure S3(d). If Tb₂O₃ (Tb = 100%) is used, it is certain
 105 that the magnet volume can be further reduced as the work is in progress. Principally, when Tb₂O₃
 106 sample with same length as the TGG crystal is used, the required magnet volume can be reduced in
 107 accordance with the largeness of the Verdet constant. But for practical use in optical isolator, it cannot
 108 be reduced to 1/4 because of the actual distribution of magnetic flux density of magnet housing. For
 109 industrial application, issues on downsizing and low cost are very important. By using these ceramic
 110 Faraday rotators with highest Verdet constant, it is possible to overcome the weak points of the
 111 conventional technology by single crystal materials.



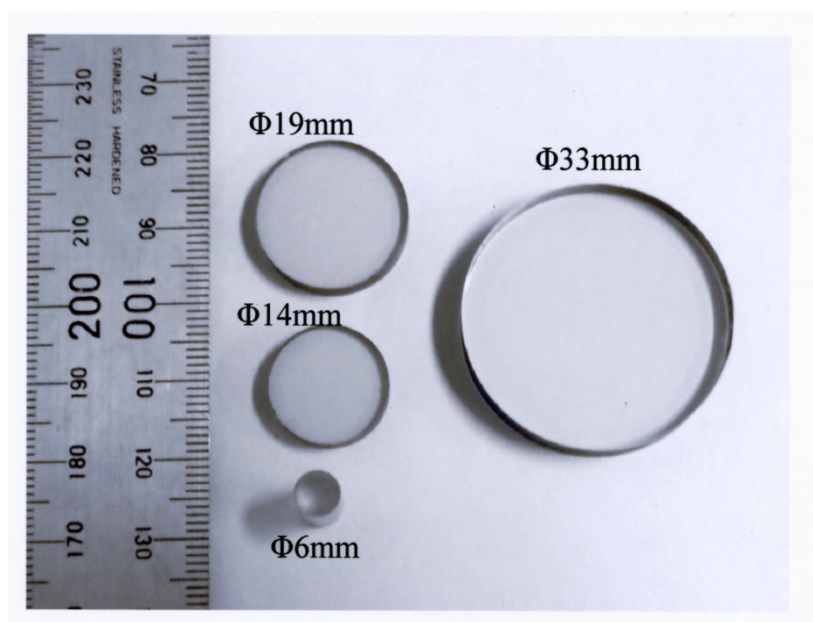
112

113 **Figure S3.** (a) Prototype of optical isolator using TYO (Tb-60%) ceramic in comparison with
 114 commercial TGG optical isolator. (b) Schematic diagram of optical isolator. (c) Magnetic flux
 115 distribution inside the magnet house of optical isolator and the position of Faraday rotator sample
 116 influenced by the magnetic field. (d) Comparison of features of each Faraday rotator material.

117 Demonstration of Large Aperture Ceramic Isolator for High Power Laser

118 Good reproducibility and productivity were achieved in this work, which are better than the
 119 case of single crystal, with ceramic fabrication technology. For example, in the case of sample with Φ
 120 6 mm \times 10 mm dimension, it is possible to produce several thousands to ten thousands of pieces per
 121 batch. Samples with 5 mm diameter described above are normally usable for laser power up to 100
 122 W class. For kW class high-power laser operations, Faraday rotator element with large aperture
 123 ($\Phi 10\text{--}15\text{mm}$) are required. For application in nuclear fusion and high energy physics in the future,
 124 samples with larger aperture ($\Phi 20\text{--}50$ mm) will become indispensable. With the invention from this
 125 work, it was successful to produce large samples with good transparency (see Figure S4). The work
 126 on the development of large scaled samples with improved optical quality is in progress, and it is
 127 still necessary to achieve good laser damage performance of large samples higher than the TGG
 128 reference. We have confirmed that the laser damage property of the TYO ceramics significantly
 129 exceeded the value of TGG but the details of their laser damage properties will be reported in another
 130 paper in near future.

131 Production style of ceramic is different from that of single crystal. In the case of single crystal, a
 132 relatively large size crystal is produced and then it is cut and machined to get required smaller size
 133 elements. In the case of ceramic, they can be produced in near net shaping to the required size and in
 134 large quantity. Therefore, ceramic production style is more favorable than that of single crystal.



135

136

Figure S4. Appearance of large scaled TYO ceramic samples with various aperture sizes.

137 Figure Captions

138 Figure S1. (a) External view, and (b) polarized optical microscopic image of $(\text{Tb}_{0.5}\text{Y}_{0.5})_2\text{O}_3$ single
139 crystal.

140 Figure S2. Relationships between the Tb ion concentration and the refractive index, and the thermal
141 conductivity.

142 Figure S3. (a) Prototype of optical isolator using TYO (Tb-60%) ceramic in comparison with
143 commercial TGG optical isolator. (b) Schematic diagram of optical isolator. (c) Magnetic flux
144 distribution inside the magnet house of optical isolator and the position of Faraday rotator sample
145 influenced by the magnetic field. (d) Comparison of features of each Faraday rotator material.

146 Figure S4. Appearance of large scaled TYO ceramic samples with various aperture sizes.

147



© 2019 by the authors. Submitted for possible open access publication under the terms
and conditions of the Creative Commons Attribution (CC BY) license
(<http://creativecommons.org/licenses/by/4.0/>).

148